PCCP

ROYAL SOCIETY OF CHEMISTRY

PAPER

View Article Online
View Journal | View Issue

Cite this: *Phys. Chem. Chem. Phys.*, 2021, **23**, 10988

The effect of introducing Ga on the ZSM-5-catalyzed methanol to aromatics reaction: taking methylcyclopentane to benzene as an example†

Dandan Zhang,[a] Hongyan Liu,*[ab] Lixia Ling,[ac] Hairong Zhang,[ab] Riguang Zhang,[a] Ping Liu[d] and Baojun Wang*[a]

Received 5th November 2020,
Accepted 19th March 2021

DOI: 10.1039/d0cp05778a

rsc.li/pccp

Naphthenes are key intermediates in the formation of aromatic compounds during the methanol to aromatics (MTA) reaction, and the dehydrogenation process is more important than the hydrogen transfer process. Theoretical studies were performed to investigate the methylcyclopentane, which represents a naphthene, to benzene MTA process catalyzed by ZSM-5 before and after introducing Ga, showing that Ga-ZSM-5 was more favorable for carrying out the reaction than two H-type ZSM-5 (H-Z_1 and H-Z_2) models. H-Z_1 and H-Z_2 are favorable for the transfer of H during ring expansion reactions and the reformation of Brønsted acids, but the dehydrogenation reactions involving H-Z_1 and H-Z_2 require high free-energy barriers to be overcome. Although introducing Ga to ZSM-5 is not conducive to the transfer of H after dehydrogenation, it can reduce the extremely high dehydrogenation free-energy barrier compared with H-Z_1 and H-Z_2; this is mainly because Ga at dehydrogenation active centers, $[GaH]^{2+}$, can accept electrons and donate them to the H atoms of $[GaH]^{2+}$, giving H negative charge and making it easy to combine with positive B-acid H atoms that come from methylcyclopentane, cyclohexene, and cyclohexadiene to produce H_2. Also, analysis of the transition state structures of all DH processes shows that Ga-ZSM-5 is more favorable for promoting the combination of H to produce H_2 than H-Z_1 and H-Z_2.

1. Introduction

Aromatics, especially benzene, toluene, and xylene (BTX), are basic raw materials in the organic chemical and polymer industries, and they are widely used in medicines, spices, fuels, dyes, *etc.*[1–3] However, the production of aromatics seriously depends on petroleum; moreover, shortages of petroleum reserves and the sharp increase in the demand for aromatics have raised interest in the production of aromatics through non-petroleum routes. At present, the methanol to aromatics (MTA) process has attracted great attention, as the reactant methanol can be obtained from various carbon-based feedstocks, such as coal, natural gas, and biomass, instead of petroleum.[4,5] Unfortunately, low aromatic yields and BTX selectivity are the main limiting factors that hinder the industrial application of MTA.

MTA is a very complex process, mainly involving dehydration, oligomerization, cyclization, hydrogen transfer, and dehydrogenation (DH) reactions. During the MTA process, light olefins (mainly ethylene and propylene), which come from methanol, are converted to naphthenes *via* oligomerisation and cyclization.[6,7] Previous studies investigated the oligomerization and cyclization of ethylene, propene, and linear C_5, C_6 and C_7 olefins, indicating that methylcyclopentane and methylcyclohexane could be readily formed;[8,9] then, the formed naphthenes can produce aromatics *via* hydrogen transfer or DH.[10]

ZSM-5 is widely used as a catalyst in MTA reactions because of its advantages of high-temperature resistance, easily modified acidity, and good shape selection for aromatics.[11–13] It is noted that aromatic selectivity was only 30–40% when catalyzed by pure ZSM-5 without metal modification, and this was accompanied by a large amount of undesired alkanes, mainly through hydrogen transfer.[14–16] However, the formation of aromatics increased obviously when promoted by ZSM-5 with metal modification.[17] For example, metals (Zn, Ga, Ag, *etc.*) were introduced to ZSM-5

[a] *Key Laboratory of Coal Science and Technology of Ministry of Education and Shanxi Province, Taiyuan University of Technology, No. 79 Yingze West Street, Taiyuan 030024, Shanxi, P. R. China. E-mail: liuhongyan@tyut.edu.cn, wangbaojun@tyut.edu.cn*
[b] *College of Chemistry and Chemical Engineering, Shanxi Datong University, Datong 037009, Shanxi, P. R. China*
[c] *College of Chemistry and Chemical Engineering, Taiyuan University of Technology, Taiyuan 030024, Shanxi, P. R. China*
[d] *State Key Laboratory of Coal Conversion, Institute of Coal Chemistry, Chinese Academy of Sciences, Taiyuan 030001, P. R. China*

† Electronic supplementary information (ESI) available. See DOI: 10.1039/d0cp05778a

to improve the aromatic selectivity.[18–20] Pinillaherrero *et al.*[21] investigated the effects of Zn in ZSM-5 on the MTA reaction: the results showed that Zn increased the aromatic yields *via* promoting the DH process. Also, Niu *et al.*[22] found that Zn species significantly improved the aromatic selectivity and played an essential role in enhancing the DH of alkanes and the aromatization of alkenes. In addition, according to an experimental report by Inoue *et al.*,[20] the aromatic yield can reach 80% when using Ag-ZSM-5, much higher than that over pure H-ZSM-5 (43%). Ga-ZSM-5 has been used for the aromatization of liquefied petroleum gas alkanes.[23–25] It was also used in MTA reaction research to increase aromatic yields. Gao *et al.*[19,26] investigated the DH process during the MTA reaction over Ga-modified ZSM-5 zeolites, indicating that the cyclic intermediates were readily cracked on Brønsted acid sites (BASs), and the prevailing hydrogen transfer process resulted in low selectivity for aromatics on H-ZSM-5. However, when Ga species were formed *via* the substitution of BASs on H-ZSM-5, the conversion of C_5 and C_6 cycloalkenes to aromatics was favored *via* the promotion of the DH over Ga-ZSM-5. Also, the authors analyzed the product distribution and the results showed that a large amount of H_2 was produced on Ga-ZSM-5, while only a very small amount of H_2 was present on H-ZSM-5. Therefore, it is necessary to analyze the role of Ga-ZSM-5 in the DH process in more detail. In addition, extra-framework Ga species are essential for promoting the aromatic yields in MTA, which was proved by Hsieh *et al.*,[27] and this is mainly related to synergy between the BASs and extra-framework Ga species to promote DH. In short, the introduction of specific metals to ZSM-5 can promote the DH process and increase aromatic yields. Unfortunately, the role of the addition of metals to ZSM-5 and detailed mechanisms are unclear. It is necessary to clarify this and provide some information for the experimental preparation of better modified ZSM-5 catalysts for the MTA reaction.

Based on previous investigations, it can be found that methylcyclopentane and methylcyclohexane are easy to form.[8,9] Methylcyclopentane and methylcyclohexane can generate aromatics through hydrogen transfer or dehydrogenation. Hydrogen transfer means moving a hydrogen atom from one olefin/carbocationic intermediate to another. It was reported that dehydrogenation through hydrogen transfer on Y zeolites shows significantly lower barriers than unimolecular dehydrogenation,[28] but the pore size of ZSM-5 is too small for bimolecular hydrogen transfer reactions to occur.[29] Therefore, in this work, methylcyclopentane to benzene is used as an example to represent naphthene to aromatics reactions in order to investigate the effects of the addition of Ga to ZSM-5 on the DH process; this can also further clarify the effects of the addition of Ga to ZSM-5 on MTA. Therefore, the reaction mechanism of methylcyclopentane to benzene was investigated on H-ZSM-5 and Ga-ZSM-5 using the density functional theory (DFT) method. This is expected to clarify the effects on the reaction from an electronic-level perspective over H-ZSM-5 and Ga-ZSM-5 and to provide theoretical guidance for finding good MTA catalysts to promote the formation of aromatics.

2. Computational details

2.1 Model

ZSM-5 has 12 crystallographically nonequivalent tetrahedral (T) sites, and the framework consists of tetrahedral T (Si or Al) atoms that are surrounded by oxygen atoms. When all T atoms are Si, the framework is electronically neutral, and when the Si atoms are partially replaced by Al atoms, bridged hydroxyl groups (Al–OH–Si) are formed as Brønsted (B) acids. In our work, ZSM-5 is represented by a 72T cluster model, which contains complete double 10-membered ring intersection pores of straight and zigzag channels.[30] The 72T cluster model not only contains intersection cavities between the straight and sinusoidal channels, which are the main catalytically active centers for catalytic reactions but it is also suitable when considering computation costs. The terminations of the 72T cluster are saturated by H atoms, and the Si–H distance is fixed at a bond length of 1.47 Å, oriented along the direction of the corresponding Si–O bond.[30,31] There are T sites in H-ZSM-5 that show better binding and adsorption abilities, *e.g.*, T6 sites,[32] but we adopt T12 as the active site because the T12 site is located at the intersection of straight and zigzag channels. It is the most likely to be substituted and is considered to be one of the most active sites in ZSM-5; also, it can provide the largest space for hydrocarbon conversion.[33–35] Al_{12}–O_{32}H–Si_3 is chosen as the researched BAS, and it is the most accessible active site for molecules.[36] In order to ensure that the studied H-ZSM-5 and Ga-ZSM-5 models have the same framework structures, another Al atom replaces Si_3, which is located on the same 10-membered ring as T12. The corresponding models are shown in Fig. 1.

For H-ZSM-5, to maintain electrical neutrality in the calculated models, it is considered that another H proton, which is not considered to be an active site, is located on O_{14} or O_{32}, respectively; the created models are correspondingly denoted as H-Z_1 and H-Z_2. When Ga was added to ZSM-5, Rane *et al.*[37] characterized the properties of different forms of active Ga species and found that Ga^+ has excellent performance in terms of stability, regeneration ability, and the promotion of propane

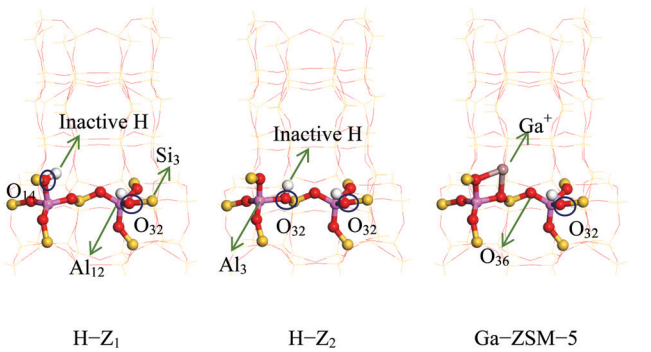

Fig. 1 Models of H-Z_1, H-Z_2, and Ga-ZSM-5. Atoms shown with balls and sticks were treated with the high-level DFT method, while the rest of the frameworks shown with lines were treated with the low-level method, calculated using pm6 (Al: pink, Si: yellow, O: red, H: white, and Ga: brown).

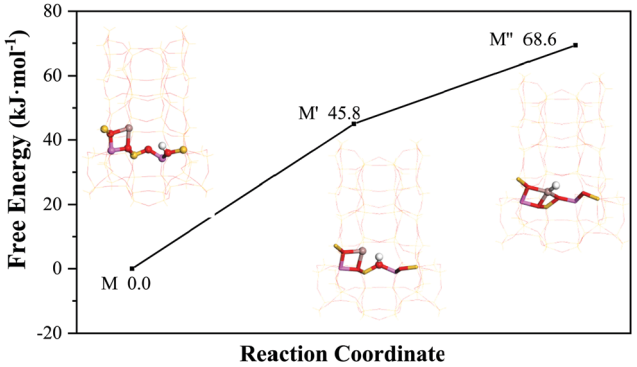

Fig. 2 The optimal model and free energies of B-acid proton transfer from a BAS to Ga^+ on Ga-ZSM-5.

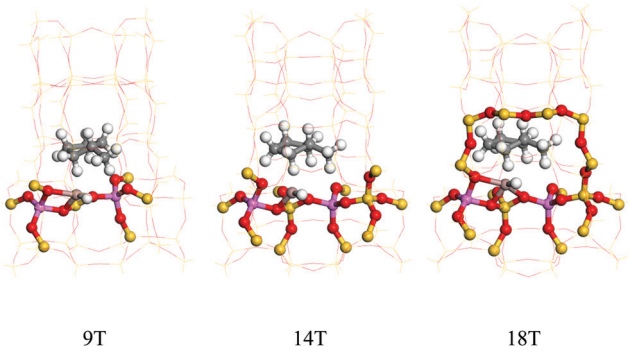

Fig. 3 The adsorption of methylcyclopentane on three high-level Ga-ZSM-5 layer models involving 9T, 14T, and 18T.

dehydrogenation. Also, extra-framework Ga plays a vital role in the formation of aromatics, which was formed *via* substituting B-acid protons.[27,38] Therefore, in this work, extra-framework active Ga species are obtained *via* replacing the H protons on O_{14} of H-Z_1 and on O_{32} of H-Z_2 with Ga.

Schreiber *et al.*[38] indicated that B-acid protons can be transferred to Ga^+ to form $[GaH]^{2+}$, which was the active center of propane dehydrogenation, so the migration energy of B-acid protons is calculated in our work. The optimal model and migration free energies of Ga-ZSM-5 in this work are shown in Fig. 2. The transfer of a B-acid proton from a BAS to Ga^+ undergoes two steps: M → M′ and M′ → M″, with M′ and M″ being 45.8 and 68.6 kJ mol^{-1} higher in free energy than M, which is similar to the study of Schreiber *et al.*[38] In summary, the low B-acid proton migration energy means that $[GaH]^{2+}$ is easily formed and can be used as the active center. In addition, Phadke *et al.*[39] pointed out through phase diagram calculations that $[GaH]^{2+}$ cations appear to be stable at all tested H_2 partial pressures when the framework Al atom is located as the next-nearest neighbor at temperatures >623 K. Even at very low H_2O partial pressures (10^{-1} Pa), $[GaH]^{2+}$ cations are still the most stable structures in the presence of H_2. Joshi *et al.*[40] concluded that the activities of $[GaH]^{2+}$ sites are less sensitive to temperature. Mansoor *et al.*[41] researched the relative stabilities of some Ga species and their activities for the DH of light alkanes, proving $[GaH]^{2+}$ to be the most active site for the DH of light alkanes. In this work, the following investigation is based on the $[GaH]^{2+}$ model of M″ given in Fig. 2.

2.2 Methods

All calculations were performed with the Gaussian 09 package. A combined theoretical approach, namely ONIOM (ωb97xd/6-31G(d,p):pm6), was used for the geometry optimization of adsorption states and transition states (TS). As shown in Fig. 1, the active-site atoms were treated as the high-level layer, and the rest of the framework as the low-level layer. In order to ensure the accuracy of the results, we tested the adsorption of methylcyclopentane on three high-level layer Ga-ZSM-5 models, 9T, 14T, and 18T, as shown in Fig. 3. The adsorption energies of methylcyclopentane on the three models are −176.2, −178.2, and −181.5 kJ mol^{-1}, respectively. Obviously, the difference is small and almost negligible. To save computing resources, we use the model with the high-level layer of 9T in the following calculations. In this work, transition states (TS) were estimated using the OPT = TS method and confirmed *via* the quasi-internal reaction coordinate (quasi-IRC) approach to verify that each transition state was connected with the corresponding reactants and products. Then, based on the imaginary vibrational model of the optimized TS, the positions of the vibrational atoms were slightly adjusted along the calculated reaction coordinate in two directions, toward the reactant and the product, respectively, and, finally, the resulting structure was optimized to the stable state. Although the ONIOM method can describe the structure of an adsorbed species well, it will introduce a large calculation error at the junction of the high- and low-level layers.[42,43] To correct this, the ωb97xd hybrid density functional, including dispersion interactions, combined with the 6-31G(d,p) basis set was employed to recalculate the energies, and thermal energies were corrected at 298 K for the geometries obtained *via* the ONIOM method. Because the activities of $[GaH]^{2+}$ sites are less sensitive to temperature,[40] we only calculate the free energy at 298 K without considering other temperatures in this article. The free energy barrier was defined as the energy difference between the reactant and transition state (TS), and the reaction free energy was the energy difference between the reactant and product in an elementary reaction.

3. Results and discussion

3.1 Methylcyclopentane to benzene

The methylcyclopentane to benzene reaction mainly includes the following steps: methylcyclopentane to cyclohexene, cyclohexene to cyclohexadiene, and cyclohexadiene to benzene; furthermore, the formation of cyclohexene from methylcyclopentane involves primary, secondary, and tertiary carbon mechanisms. The detailed mechanistic routes catalyzed by ZSM-5 before and after the introduction of Ga are shown in Schemes 1 and 2, respectively. Additionally, Fig. 4 shows the structures of methylcyclopentane, cyclohexene, and cyclohexadiene; the H and C atoms involved in the reaction process are marked with letters as subscripts. The dehydrogenation process

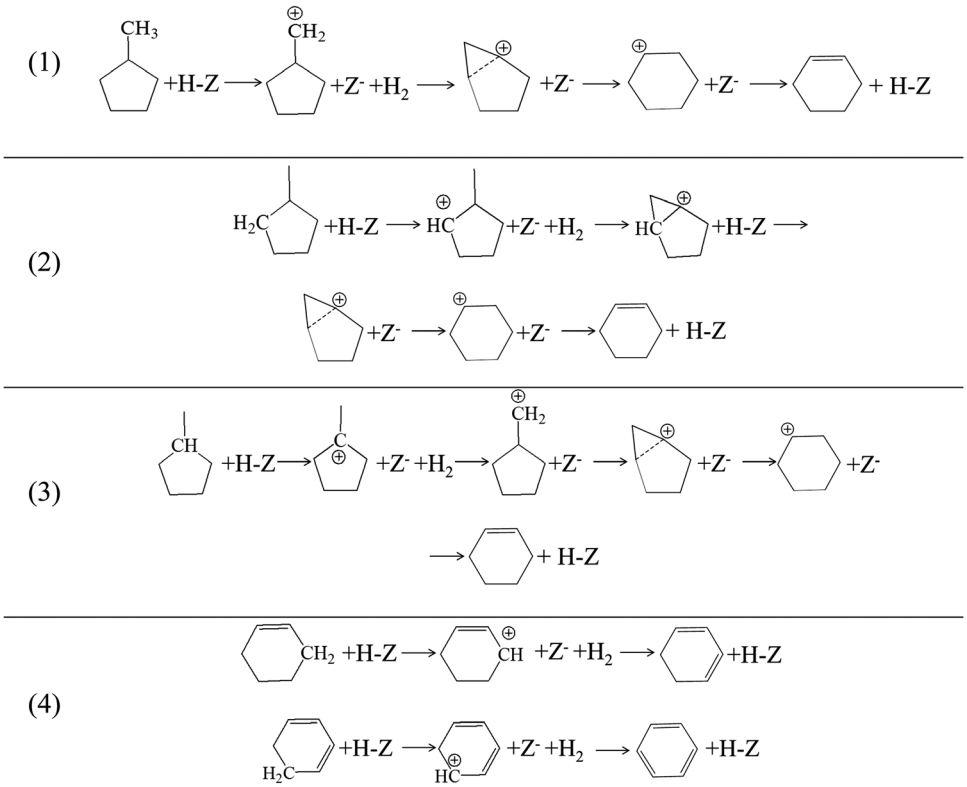

Scheme 1 Schematic diagrams of methylcyclopentane to cyclohexene processes *via* primary carbon (1), secondary carbon (2), and tertiary carbon (3) mechanisms and the cyclohexene to benzene (4) process on H-ZSM-5.

proposed in previous reports[19,38] involves the transfer of H atoms between the reactant and ZSM-5, which is represented by HT in this paper.

3.1.1 Methylcyclopentane to cyclohexene. The methylcyclopentane to cyclohexene process involves DH and a ring expansion reaction, which will start from primary carbon, secondary carbon, or tertiary carbon in methylcyclopentane.[44,45] As shown in Fig. 4a, C_1, C_3, and C_2 are the primary, secondary and tertiary carbon atoms involved in our work, respectively. The detailed steps for the methylcyclopentane to cyclohexene process are as follows: (1) a H atom from methylcyclopentane combines with a B-acid proton from H-Z_1 and H-Z_2 or moves to the O_{36} atom of Ga-ZSM-5, and it then combines with a H atom from $[GaH]^{2+}$ to produce a carbonium ion and H_2; (2) the carbonium ion forms a 6-membered ring through ring expansion, and then loses one H atom to restore the B acid at the same time as forming cyclohexene in the three models.

Primary carbon mechanism. The potential energy plots and corresponding skeletal formulae for the production of cyclohexene from methylcyclopentane through a primary carbon mechanism on H-Z_1 and H-Z_2 are shown in Fig. 5 and 6. The geometric structures are shown in Fig. S1 and S2 (ESI†). From P-A to P-B and P-A′ to P-B′, DH processes occur on H-Z_1 and H-Z_2. In these processes, the H_a atoms bonded with C_1 in methylcyclopentane combine with a B-acid proton through P-TS1 and P-TS1′ to generate H_2; at the same time, H_c is transferred to C_1 to generate tertiary carbonium ions (P-B and P-B′). Because of space constraints, the carbonium ions bond with O_{36}. These elementary reactions require activation free energies of 283.0 and 260.7 kJ mol^{-1}. Subsequently, from P-B to P-E and P-B′ to P-E′, ring expansion occurs through HT and the structures change; the H_c atom is transferred to the tertiary carbon *via* P-TS2 and P-TS2′, in which the reactants overcome free energy barriers of 90.2 and 57.5 kJ mol^{-1} to form primary carbonium ions (P-C and P-C′), which bonded with O_{32}. Then, the structures of the primary carbonium ions change, and the C_1 and C_3 atoms are bonded together through the intermediates P-D and P-D′, undergoing ring expansion reactions to generate cyclohexane carbonium ions (P-E and P-E′), in which C_2 is bonded with O_{36}; these steps need activation free energies of 62.7 and 25.4 kJ mol^{-1}. Finally, from P-E to P-F and P-E′ to P-F′, B-acid sites and cyclohexene are formed *via* HT, *i.e.*, the cyclohexane carbonium ions lose H_d through P-TS3 and P-TS3′, overcoming free energy barriers of 65.4 and 54.9 kJ mol^{-1}, to generate a B acid and cyclohexene (P-F and P-F′).

For Ga-ZSM-5, the process from methylcyclopentane to cyclohexene is different from those on H-Z_1 and H-Z_2, as shown in Fig. 7. The geometric structures are shown in Fig. S3 (ESI†). Firstly, HT occurs, going from P-A″ to P-B″. The H_a atom of C_1 is transferred to the O_{36} position of Ga-ZSM-5 *via* P-TS1″ to form a new B-acid proton and a primary carbonium ion bonded with Ga (P-B″); this process requires free energy of 51.9 kJ mol^{-1}. Then, DH occurs, going from P-B″ to P-C″; the new B-acid proton is combined with a H atom of $[GaH]^{2+}$ through P-TS2″ to

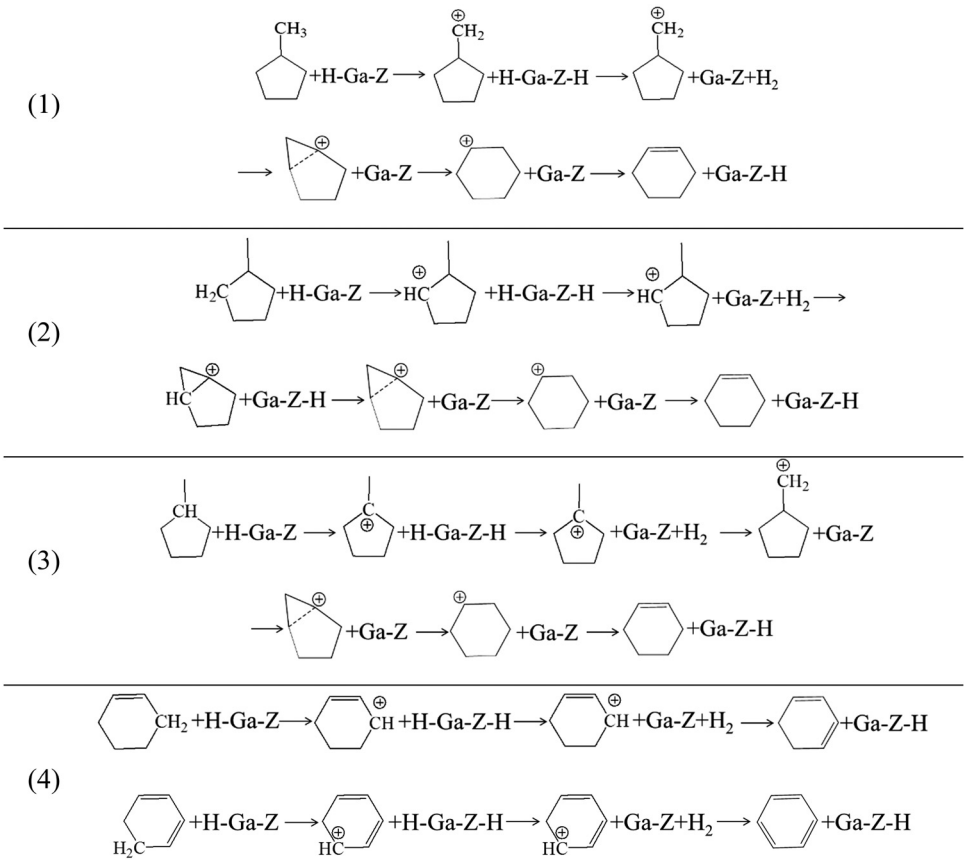

Scheme 2 Schematic diagrams of methylcyclopentane to cyclohexene processes *via* primary carbon (1), secondary carbon (2), and tertiary carbon (3) mechanisms and the cyclohexene to benzene (4) process on Ga-ZSM-5.

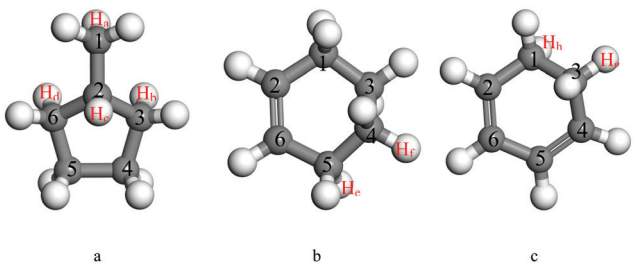

Fig. 4 The structures of methylcyclopentane, cyclohexene, and cyclohexadiene, and the atoms involved in the reaction processes.

eliminate H_2 (P-C″), which needs to overcome a free energy barrier of 76.2 kJ mol^{-1}. From P-C″ to P-E″, a ring expansion reaction occurs; the structure of the primary carbonium ion changes and ring expansion occurs *via* P-D″, which needs an activation free energy of 99.3 kJ mol^{-1} to form a cyclohexane carbonium ion (P-E″) bonded with Ga. Finally, from P-E″ to P-F″, a B-acid site and cyclohexene are formed *via* HT; H_d transfers to the O_{32} site *via* P-TS3″, overcoming a free energy barrier of 123.3 kJ mol^{-1} to restore the BAS and produce cyclohexene (P-F″).

Based on these results, it can be clearly seen that the highest free energy barriers required on H-Z_1 and H-Z_2 for the production of cyclohexene *via* the primary carbon mechanism are the DH processes, with activation free energies of 283.0 and 260.7 kJ mol^{-1}, respectively, *i.e.*, the DH processes are the rate-limiting steps on H-Z_1 and H-Z_2. In addition, it is slightly easier to generate cyclohexene from methylcyclopentane on H-Z_2 through the primary carbon mechanism than on H-Z_1. The highest free barrier is 136.8 kJ mol^{-1} on Ga-ZSM-5; different from on H-Z_1 and H-Z_2, it is not the process of DH but the process of HT, involving H_d of the cyclohexane carbonium ion transferring to the zeolite, that is the rate-limiting step. It is noted that the DH free energy required is greatly reduced on Ga-ZSM-5 compared with H-Z_1 and H-Z_2. In summary, when Ga is added to ZSM-5, the highest free energy barrier is decreased, which indicates that the process of transforming methylcyclopentane to cyclohexene is easier to achieve on Ga-ZSM-5 through a primary carbon mechanism.

Secondary carbon mechanism. Cyclohexene can be produced *via* a secondary carbon mechanism on H-Z_1 and H-Z_2, and the corresponding potential energies and skeletal formulae are shown in Fig. 8 and 9. The geometric structures are shown in Fig. S4 and S5 (ESI†). From S-A to S-B and S-A′ to S-B′, DH occur on H-Z_1 and H-Z_2. H_b atoms on the C_3 atom of methylcyclopentane, *via* S-TS1 and S-TS1′, are combined with B-acid protons to form H_2 and secondary carbonium ions (S-B and S-B′) on H-Z_1 and H-Z_2; the activation free energies required are

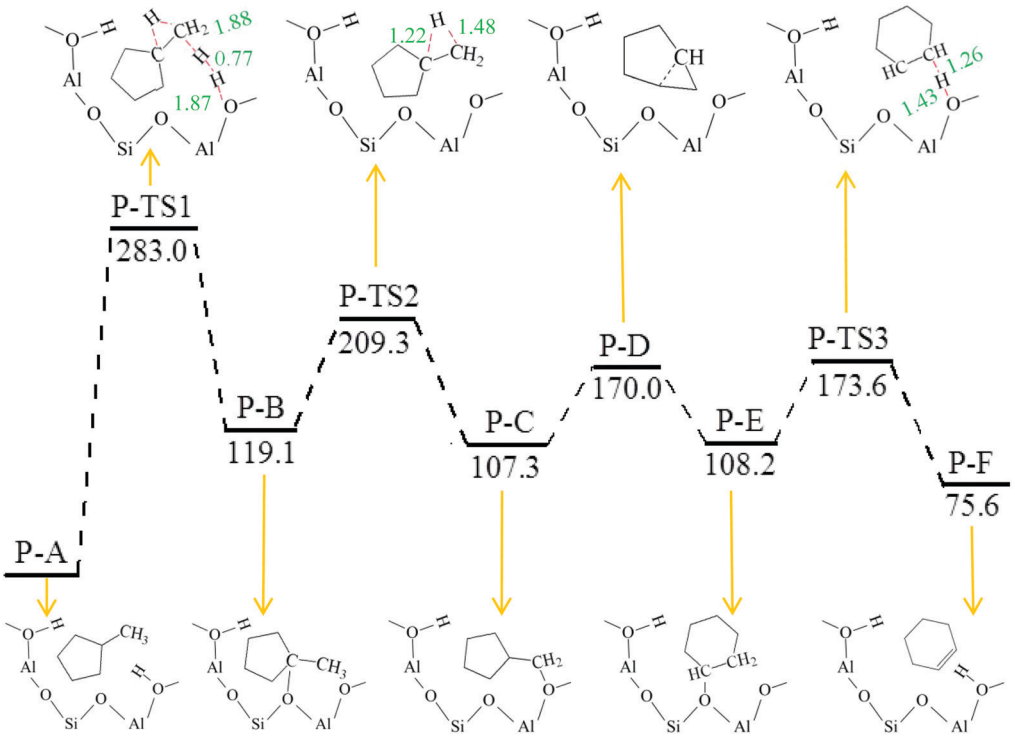

Fig. 5 The free energy barrier diagram of the methylcyclopentane to cyclohexene process through the primary carbon mechanism and the skeletal formulae of reactants, products, intermediates, and transition states on H-Z_1; all free energy values are in kJ mol^{-1}. The main geometric parameters of the transition states are also provided, and all values are in Å.

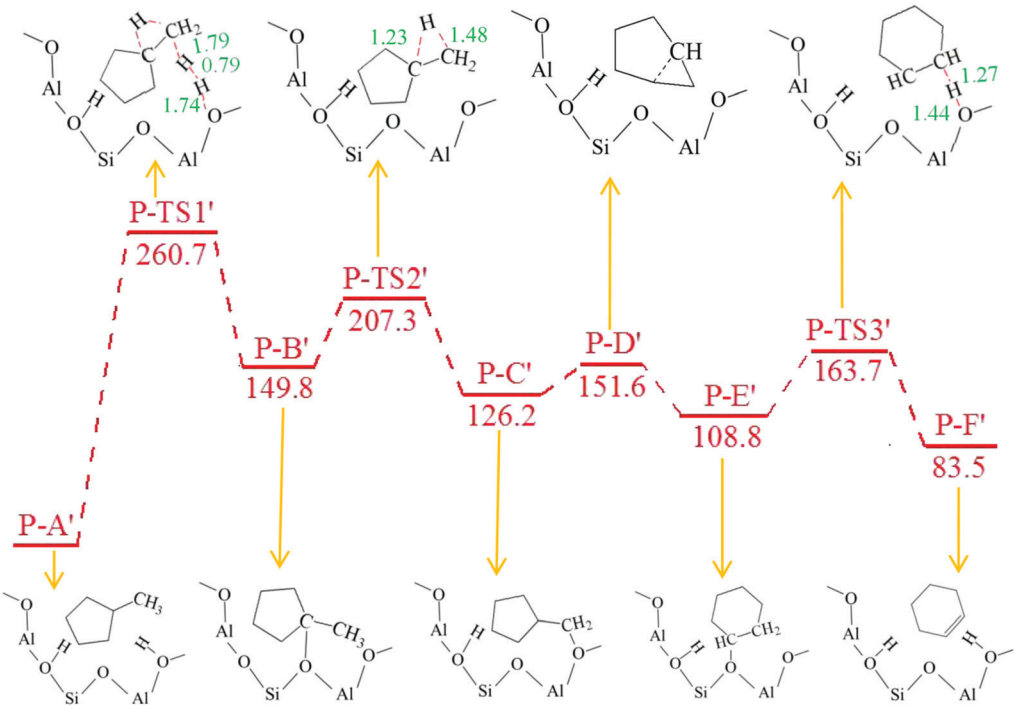

Fig. 6 The free energy barrier diagram of the methylcyclopentane to cyclohexene process through the primary carbon mechanism and the skeletal formulae of reactants, products, intermediates, and transition states on H-Z_2; all free energy values are in kJ mol^{-1}. The main geometric parameters of the transition states are also provided, and all values are in Å.

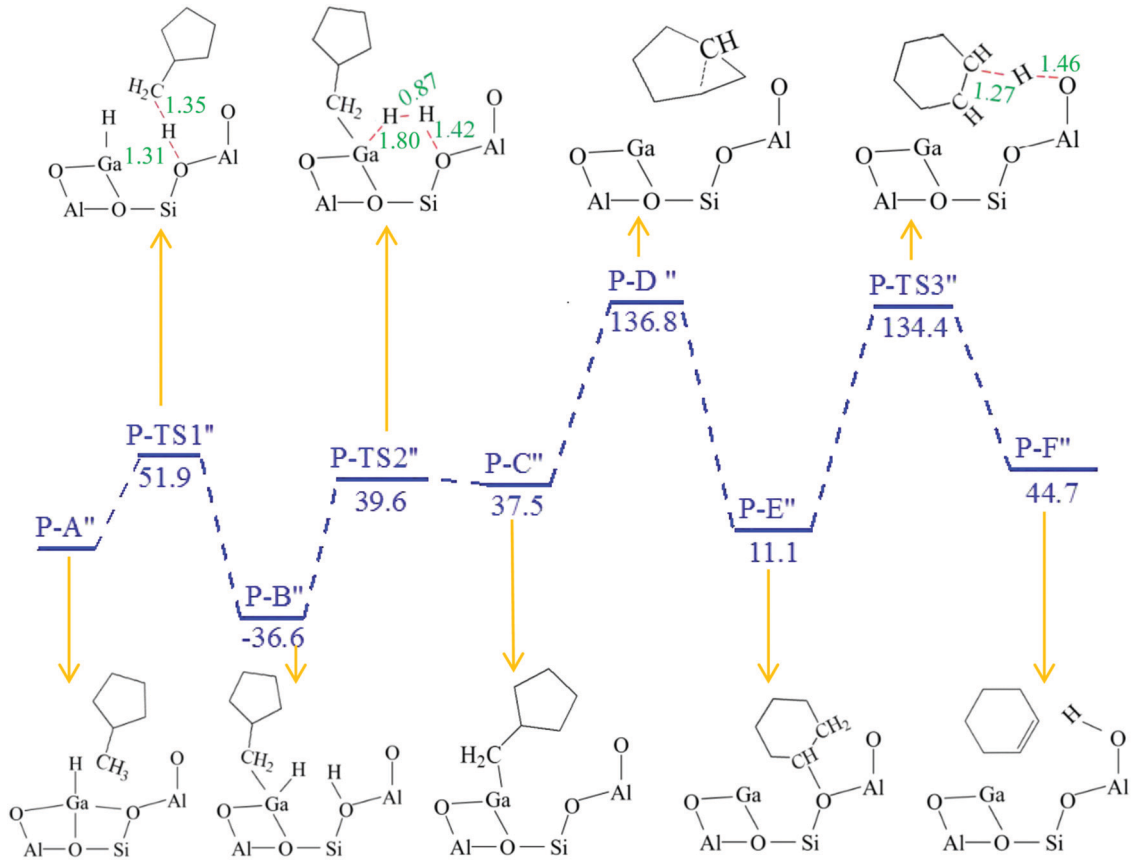

Fig. 7 The free energy barrier diagram of the methylcyclopentane to cyclohexene process through the primary carbon mechanism and the skeletal formulae of reactants, products, intermediates, and transition states on Ga-ZSM-5; all free energy values are in kJ mol^{-1}. The main geometric parameters of the transition states are also provided, and all values are in Å.

224.2 and 202.1 kJ mol^{-1}. Then, from S-B to S-E and S-B′ to S-E′, ring expansion reactions occur through HT; that is, H_a atoms of the secondary carbonium ions are transferred to O_{32} and form bicyclic intermediates (S-C and S-C′) *via* S-TS2 and S-TS2′, overcoming free energy barriers of 57.7 and 44.3 kJ mol^{-1}. The H_a atoms on O_{32}, through S-TS3 and S-TS3′, transfer to C_3 (S-D and S-D′), requiring activation free energies of 71.5 and 58.9 kJ mol^{-1}. Structure rotation and ring expansion reactions produce cyclohexane carbonium ions bonded to O_{36} (S-E and S-E′) *via* releasing free energies of 61.8 and 42.8 kJ mol^{-1}. These values are consistent with the research results of Joshi *et al.*[45] Finally, from S-E to S-F and S-E′ to S-F′, B-acid sites and cyclohexene are formed; that is, cyclohexane carbonium ions, through S-TS4 and S-TS4′, lose H_d, overcoming free energy barriers of 65.4 and 54.9 kJ mol^{-1}, to simultaneously restore BASs and form cyclohexene (S-F and S-F′).

As shown in Fig. 10, for Ga-ZSM-5, firstly, HT occurs going from S-A″ to S-B″; H_b of C_3, *via* S-TS1″, is transferred to the O_{36} site, and the required activation free energy is 68.0 kJ mol^{-1} to obtain a new B-acid proton and secondary carbonium ion adsorbed on the Ga atom (S-B″). Then, from S-B″ to S-C″, DH occurs; the new B-acid proton combines with a H atom from $[GaH]^{2+}$ through S-TS2″ to eliminate H_2 (S-C″), and this process needs to overcome a free energy barrier of 108.1 kJ mol^{-1}. Then, from S-C″ to S-F″, a ring expansion reaction occurs *via* HT; the detailed process involves H_a from the secondary carbonium ion being transferred to O_{36} to form a bicyclic intermediate (S-D″) *via* S-TS3″, which overcomes a free energy barrier of 152.6 kJ mol^{-1}. The H_a atom on O_{36}, through S-TS4″, overcomes a free energy barrier of 74.2 kJ mol^{-1} to transfer to C_3 (S-E″). After that, structure rotation and ring expansion produce a cyclohexane carbonium ion bonded to Ga (S-F″), releasing 125.7 kJ mol^{-1} of free energy. Finally, from S-F″ to S-G″, a B-acid site and cyclohexene are formed through HT; H_d is transferred to O_{32} through S-TS5″ to obtain the BAS and cyclohexene (S-G″), requiring activation free energy of 123.3 kJ mol^{-1}. The geometric structures are shown in Fig. S6 (ESI†).

According to the above results, one can see that the highest free energy barriers for cyclohexene production *via* secondary carbon on H-Z_1 and H-Z_2 are 224.2 and 202.1 kJ mol^{-1}, respectively. The corresponding processes are DH processes, which are also the rate-limiting steps. Cyclohexene generation is easier on H-Z_2 than on H-Z_1; this conclusion is consistent with that obtained based on the primary carbon mechanism. Surprising, the highest free energy barrier on Ga-ZSM-5 is the

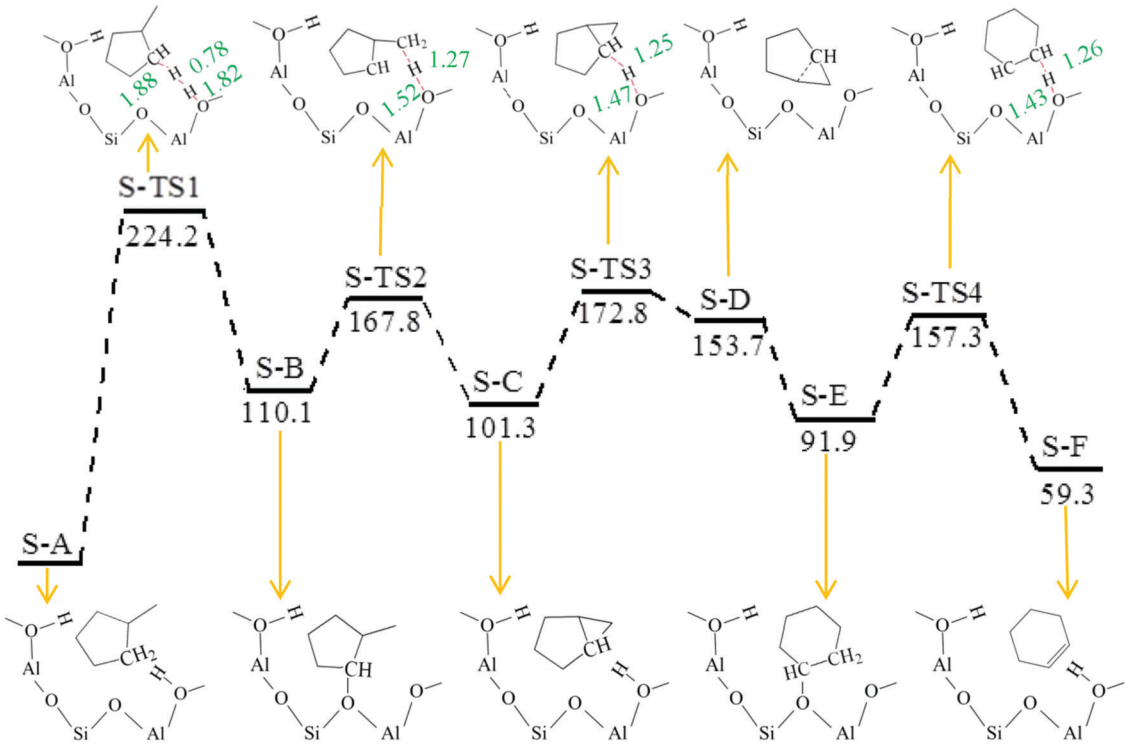

Fig. 8 The free energy barrier diagram of the methylcyclopentane to cyclohexene process through the secondary carbon mechanism and the skeletal formulae of reactants, products, intermediates, and transition states on H-Z_1; all free energy values are in kJ mol^{-1}. The main geometric parameters of the transition states are also provided, and all values are in Å.

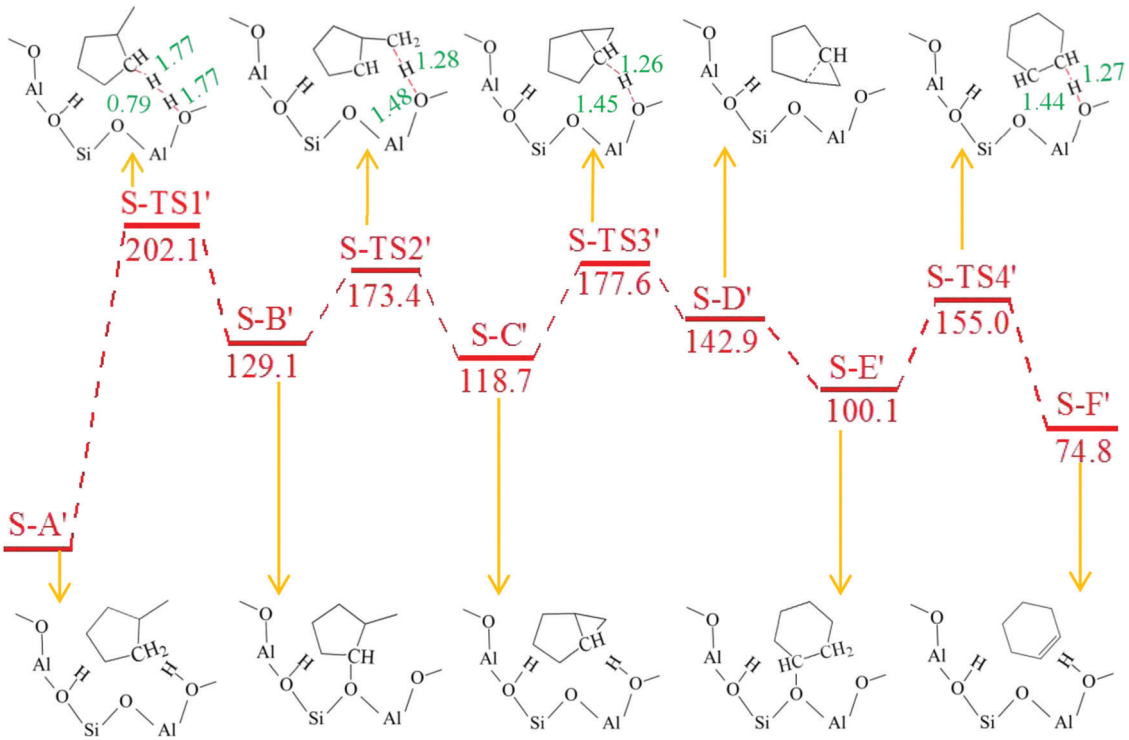

Fig. 9 The free energy barrier diagram of the methylcyclopentane to cyclohexene process through the secondary carbon mechanism and the skeletal formulae of reactants, products, intermediates, and transition states on H-Z_2; all free energy values are in kJ mol^{-1}. The main geometric parameters of the transition states are also provided, and all values are in Å.

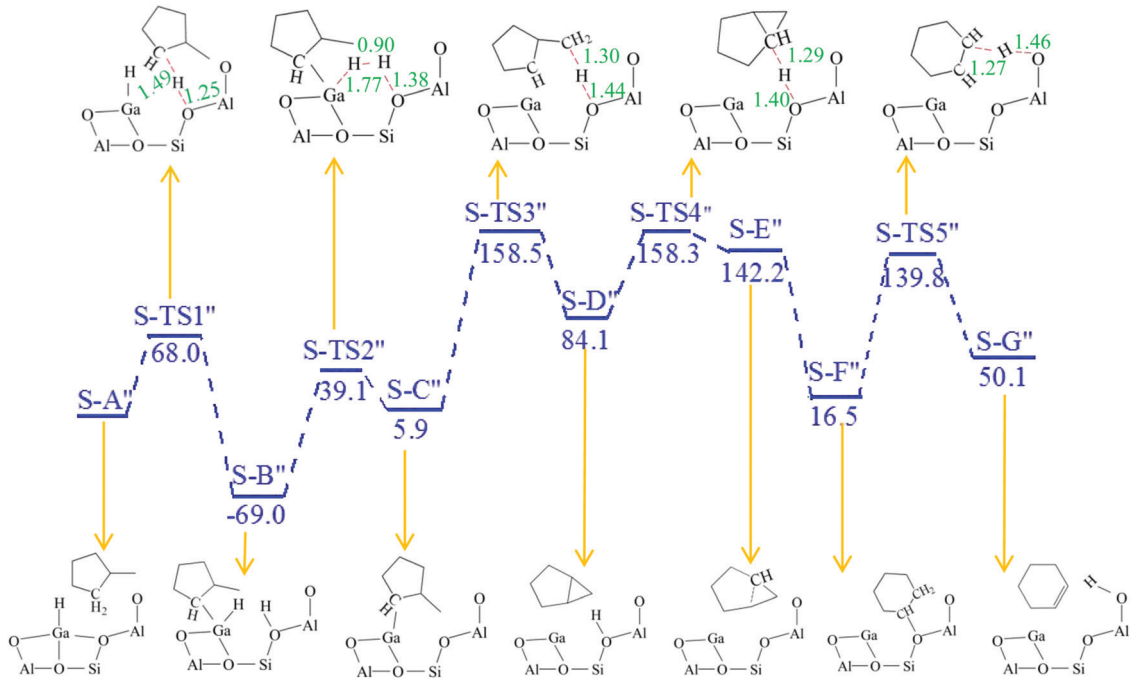

Fig. 10 The free energy barrier diagram of the methylcyclopentane to cyclohexene process through the secondary carbon mechanism and the skeletal formulae of reactants, products, intermediates, and transition states on Ga-ZSM-5; all free energy values are in kJ mol^{-1}. The main geometric parameters of the transition states are also provided, and all values are in Å.

last HT process (158.5 kJ mol^{-1}). Obviously, the introduction of Ga to ZSM-5 greatly decreases the activation free energy of DH and promotes the formation of cyclohexene, which is in accordance with the conclusions from the primary carbon mechanism.

Tertiary carbon mechanism. The potential energy profiles and corresponding skeletal formulae of the methylcyclopentane to cyclohexene process *via* tertiary carbon on H-Z_1 and H-Z_2 are shown in Fig. 11 and 12. From T-A to T-B and T-A′ to T-B′, DH occurs on H-Z_1 and H-Z_2; the H_c atoms of methylcyclopentane are combined with B-acid protons to generate H_2 and tertiary carbonium ions (T-B and T-B′) through T-TS1 and T-TS1′, and the activation free energies are 201.3 and 176.2 kJ mol^{-1}. Because of space constraints, the tertiary carbonium ions bonded with the O_{36} position. Then, from T-B to T-E and T-B′ to T-E′, ring expansion reactions occur *via* HT and the structures change. In these processes, H_a atoms are transferred to tertiary carbon *via* T-TS2 and T-TS2′ to form primary carbonium ions (T-C and T-C′), overcoming free energy barriers of 90.2 and 57.5 kJ mol^{-1}, that bond with O_{32}. Then, the primary carbonium ions overcome free energy barriers of 62.7 and 25.4 kJ mol^{-1} through the intermediates T-D and T-D′ to allow ring expansion, generating cyclohexane carbonium ions bonded to O_{36} (T-E and T-E′). These values are much smaller than those obtained in the study by Joshi *et al.*,[37] which may be caused by replacing the Si of the ZSM-5 framework with two Al atoms in this article. Finally, from T-E to T-F and T-E′ to T-F′, B-acid sites and cyclohexene are formed *via* HT, *i.e.*, the cyclohexane carbonium ions lose H_d *via* T-TS3 and T-TS3′ to restore the BASs and cyclohexene (T-F and T-F′), requiring activation free energies of 65.4 and 54.9 kJ mol^{-1}. The geometric structures are shown in Fig. S7 and S8 (ESI†).

For Ga-ZSM-5, the calculation details are shown in Fig. 13 and the geometric structures are given in Fig. S9 (ESI†). Firstly, from T-A″ to T-B″, HT occurs; that is, H_c of methylcyclopentane, *via* T-TS1″, is transferred to the O_{36} site, overcoming a free energy barrier of 47.2 kJ mol^{-1}, to produce a new B-acid proton and tertiary carbonium ion (T-B″) adsorbed on the Ga atom. Then, from T-B″ to T-C″, DH occurs; the new B acid proton is combined with a H atom from $[GaH]^{2+}$ through T-TS2″ to eliminate H_2 (T-C″), and this process requires an activation free energy of 120.7 kJ mol^{-1}. Subsequently, from T-C″ to T-F″, a ring expansion reaction occurs *via* HT and structure change; H_a is transferred to the tertiary carbon *via* T-TS3″ and then a primary carbonium ion is produced (T-D″) connected with Ga, which requires an activation free energy of 131.0 kJ mol^{-1}. The primary carbonium ion, *via* the T-E″ intermediate, forms a cyclohexane carbonium ion (T-F″), *via* overcoming a free energy barrier of 140.1 kJ mol^{-1}. Finally, from T-F″ to T-G″, a B-acid site and cyclohexene are formed through HT; the B acid of the zeolite is restored and cyclohexene (T-G″) is produced through T-TS4″, and a free energy barrier of 123.3 kJ mol^{-1} needs to be overcome.

Based on the calculations, it can be found that the highest free energy barriers on H-Z_1 and H-Z_2 are 206.6 and 198.3 kJ mol^{-1} for

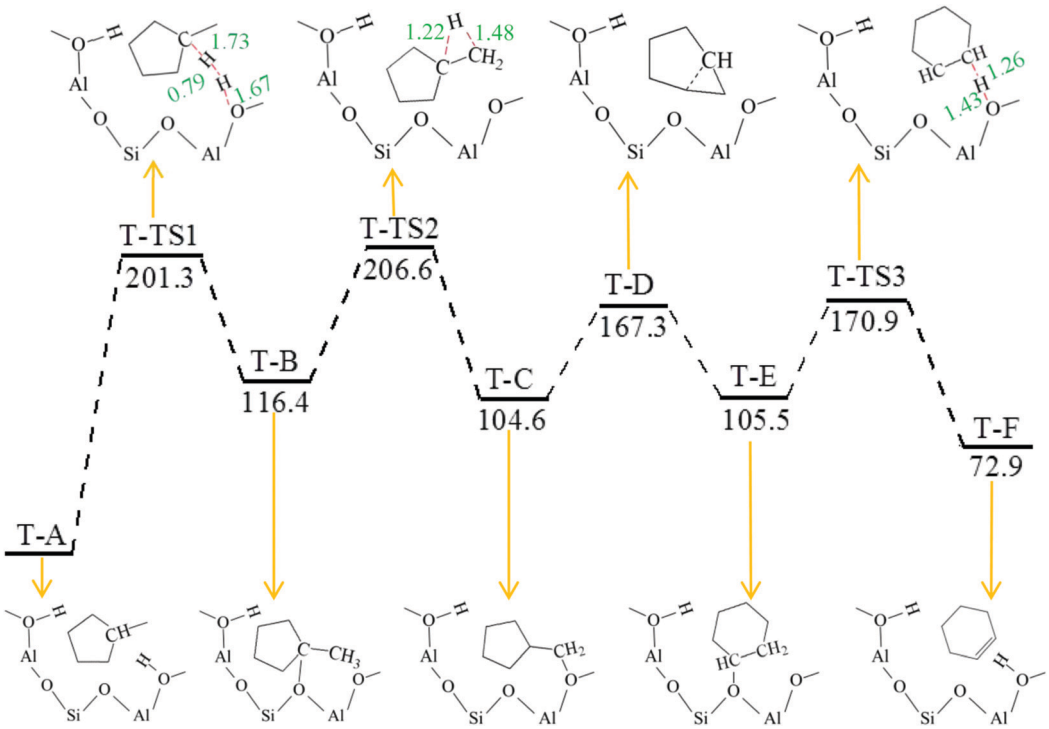

Fig. 11 The free energy barrier diagram of the methylcyclopentane to cyclohexene process through the tertiary carbon mechanism and the skeletal formulae of reactants, products, intermediates, and transition states on H-Z_1; all free energy values are in kJ mol^{-1}. The main geometric parameters of the transition states are also provided, and all values are in Å.

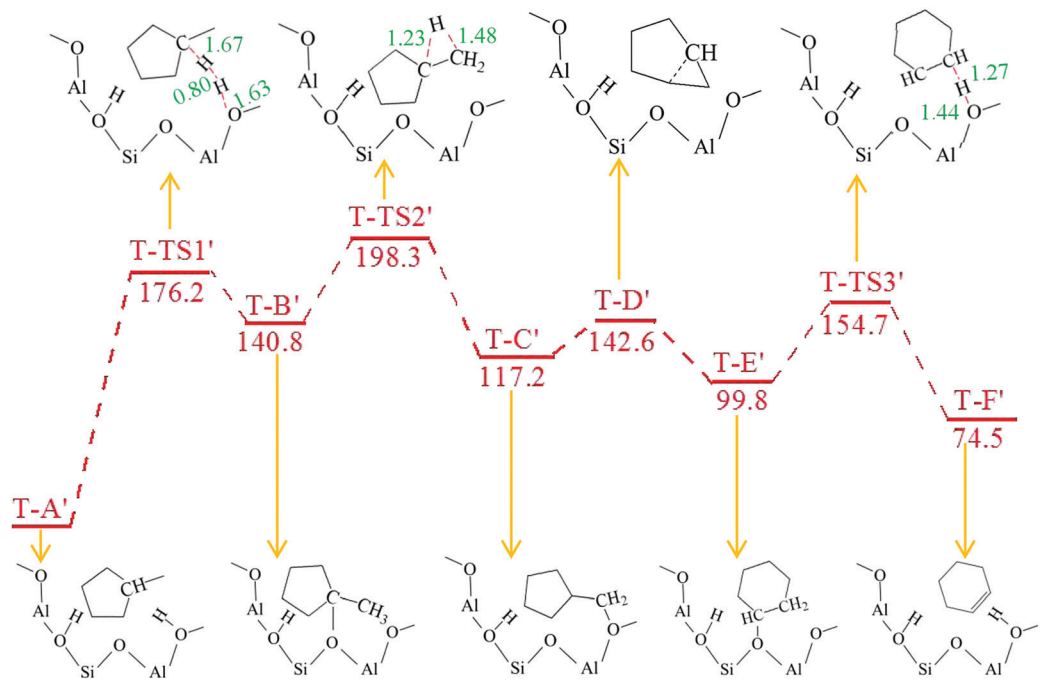

Fig. 12 The free energy barrier diagram of the methylcyclopentane to cyclohexene process through the tertiary carbon mechanism and the skeletal formulae of reactants, products, intermediates, and transition states on H-Z_2; all free energy values are in kJ mol^{-1}. The main geometric parameters of the transition states are also provided, and all values are in Å.

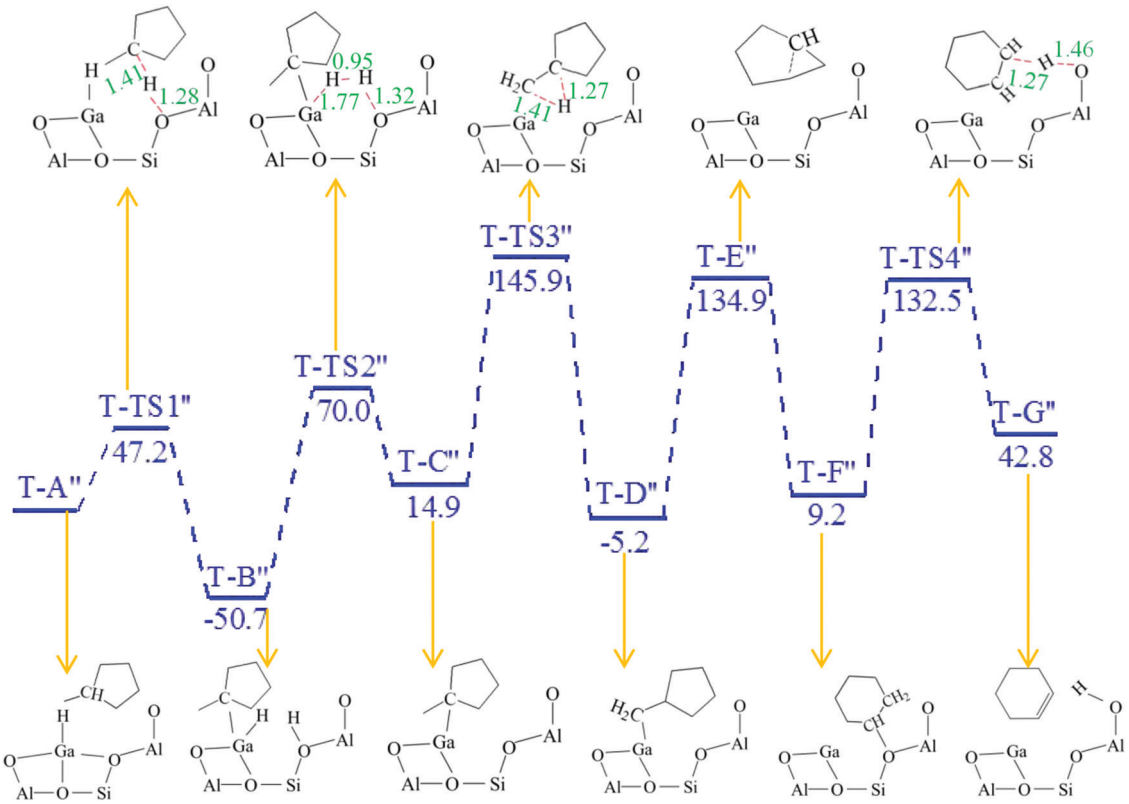

Fig. 13 The free energy barrier diagram of the methylcyclopentane to cyclohexene process through the tertiary carbon mechanism and the skeletal formulae of reactants, products, intermediates, and transition states on Ga-ZSM-5; all free energy values are in kJ mol^{-1}. The main geometric parameters of the transition states are also provided, and all values are in Å.

the methylcyclopentane to cyclohexene process *via* tertiary carbon. The DH processes are still the rate-limiting steps and cyclohexene generation is slightly easier on H-Z_2 than on H-Z_1. However, the highest free energy barrier is only 145.9 kJ mol^{-1} on Ga-ZSM-5, and the HT reaction of the tertiary carbonium ion becomes the rate-limiting step. Overall, Ga-ZSM-5 reduces the DH free energy barrier, making cyclohexene formation much more favorable than on H-Z_1 and H-Z_2 through a tertiary carbon mechanism. This result is consistent with those obtained through primary and secondary carbon mechanism studies.

3.1.2 Cyclohexene to cyclohexadiene and cyclohexadiene to benzene. Cyclohexene generated from methylcyclopentane through primary, secondary, and tertiary carbon mechanisms is rotated to a stable configuration suitable for the next reaction. The cyclohexene to benzene process undergoes two DH and two HT reactions, and the reactants, intermediates, products, and transition states involved in every elementary reaction on H-Z_1 and H-Z_2 are shown in Fig. 14 and 15. From P to Q and P′ to Q′, cyclohexene undergoes DH reactions on H-Z_1 and H-Z_2; the H_e atoms of cyclohexene (P and P′) are combined with B-acid protons to produce cyclohexene carbonium ions (Q and Q′) and eliminate H_2, overcoming free energy barriers of 203.8 and 192.1 kJ mol^{-1} through TS1 and TS1′. Next, from Q to R and Q′ to R′, the H_f atoms of the cyclohexene carbonium ions are transferred to the framework of ZSM-5 to form BASs and cyclohexadiene (R and R′) *via* TS2 and TS2′, needing to overcome free energy barriers of 44.8 and 7.9 kJ mol^{-1}. The generated cyclohexadiene rotates to a position suitable for DH, namely configurations S and S′. Then, from S to T and S′ to T′, cyclohexadiene undergoes DH reactions on H-Z_1 and H-Z_2; H_g atoms link with B-acid protons through TS3 and TS3′, and the activation free energies are 180.4 and 160.8 kJ mol^{-1} for forming H_2 and cyclohexadiene carbonium ions (T and T′). Finally, cyclohexadiene carbonium ions spontaneously lose H_h atoms to form benzene (U and U′), releasing free energies of 153.2 and 209.5 kJ mol^{-1}. The geometric structures are all shown in Fig. S10 and S11 (ESI†).

For Ga-ZSM-5, the reaction from cyclohexene to benzene is different from those on H-Z_1 and H-Z_2, as shown in Fig. 16. The detailed processes are as follows. Cyclohexene undergoes HT from P″ to Q″; H_e of cyclohexene (P″), *via* TS1″, is transferred to the O_{36} site to form a new B-acid proton and cyclohexene carbonium ion (Q″) adsorbed on the Ga atom, which requires activation free energy of 18.2 kJ mol^{-1}. Subsequently, from Q″ to R″, DH occurs; that is, a new B-acid proton is combined with a H atom from $[GaH]^{2+}$ through TS2″ to eliminate H_2, and the free energy barrier is 135.4 kJ mol^{-1}. Then, from R″ to S″, the H_f atom is transferred to O_{32} *via* TS3″ to restore the B acid and cyclohexadiene (S″), overcoming a free energy barrier of 102.9 kJ mol^{-1}. Next, cyclohexadiene

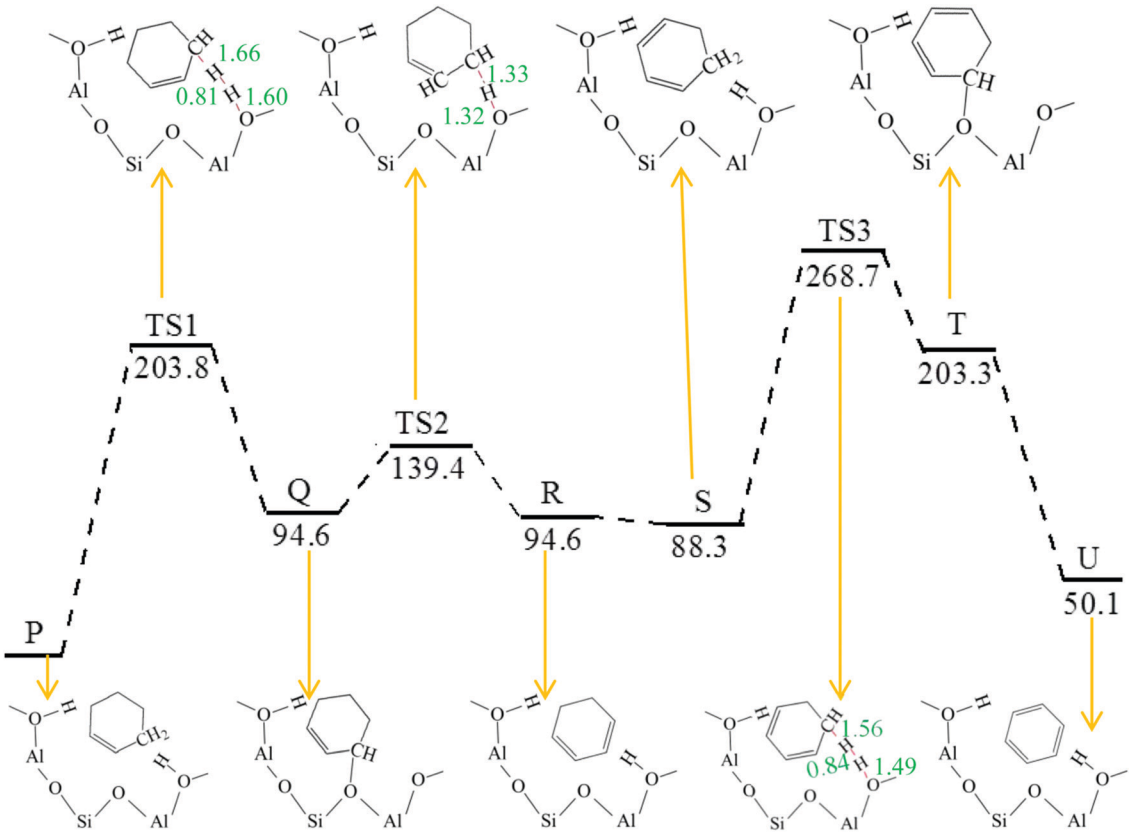

Fig. 14 The free energy barrier diagram of the cyclohexene to benzene process and the skeletal formulae of reactants, products, intermediates, and transition states on H-Z_1; all free energy values are in kJ mol^{-1}. The main geometric parameters of the transition states are also provided, and all values are in Å.

rotates to adopt configuration T″, and from T″ to U″, cyclohexadiene undergoes a HT reaction over Ga-ZSM-5, *i.e.*, the H_g atom moves to O_{36} to form a cyclohexadiene carbonium ion (U″) *via* TS4″, requiring activation free energy of 50.9 kJ mol^{-1}. Then, U″ releases H_2, through TS5″, forming V″, requiring free energy of 81.0 kJ mol^{-1}. Finally, from V″ to W″, H_g is transferred to O_{32}, which means that the B acid is restored, and the target product benzene (W″) is formed *via* TS6″, upon overcoming a free energy barrier of 116.1 kJ mol^{-1}. The geometric structures are all displayed in Fig. S12 (ESI†).

In light of the above results, it is not difficult to see that the highest barriers in the cyclohexene to benzene processes on H-Z_1 and H-Z_2 are 268.7 and 260.6 kJ mol^{-1}. DH processes are still the rate-limiting steps, and this is slightly more difficult to carry out on H-Z_1 than on H-Z_2. However, the highest barrier is 156.8 kJ mol^{-1} on Ga-ZSM-5, which is the last HT process. Comprehensively considering the cyclohexene to benzene process, we can conclude that the addition of Ga to ZSM-5 changes the mechanism and significantly reduces the activation free energy, promoting the formation of benzene.

3.2 Summary

Going from methylcyclopentane to cyclohexene and then on to benzene, the reaction processes on H-Z_1 and H-Z_2 are DH → HT → DH → HT → DH → HT, and the reaction processes are HT → DH → HT → HT → DH → HT → HT → DH → HT on Ga-ZSM-5. It can be seen that in the methylcyclopentane to cyclohexene, cyclohexene to cyclohexadiene, and cyclohexadiene to benzene processes, DH processes are always the rate-limiting steps on H-Z_1 and H-Z_2, and these reactions are slightly easier to carry out on H-Z_2 than on H-Z_1. Upon introducing Ga to ZSM-5, although the calculation results indicate that HT reactions (ring expansions or the recovery of B-acid sites) are harder to achieve on Ga-ZSM-5 than on H-Z_1 and H-Z_2, the introduction of Ga significantly reduces the free energies required for DH and, therefore, significantly promotes the formation of benzene.

3.3 Electronic structure analysis

As is well known, transition metals have the ability to accept electrons; therefore, we use CO as a probe to measure whether Ga at the DH active center of Ga-ZSM-5 has the ability to accept electrons.[46–48]

The adsorption energy of CO was calculated *via* the following equation:

$$E_{ads} = E_{Z+CO} - E_{CO} - E_Z$$

where E_{Z+CO}, E_{CO}, and E_Z denote the energies of the CO-Ga-ZSM-5 complex, isolated CO, and the Ga-ZSM-5 cluster,

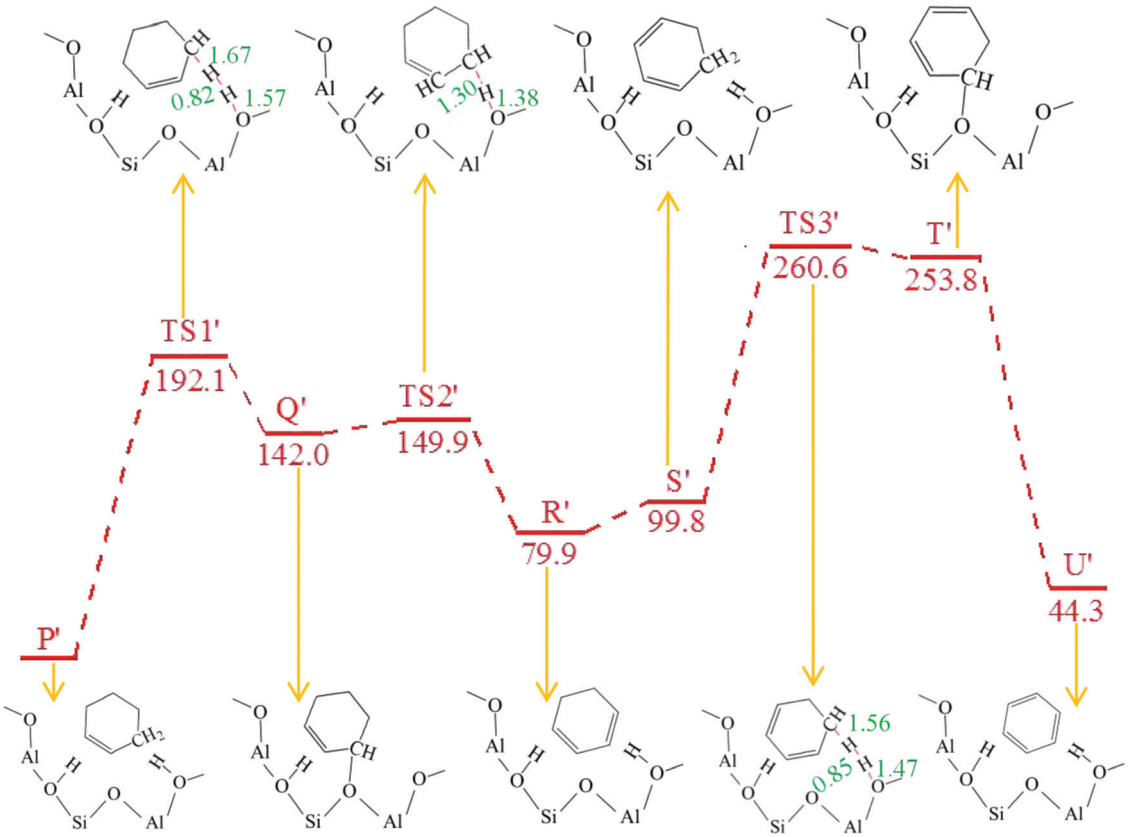

Fig. 15 The free energy barrier diagram of the cyclohexene to benzene process and the skeletal formulae of reactants, products, intermediates, and transition states on H-Z_2; all free energy values are in kJ mol^{-1}. The main geometric parameters of the transition states are also provided, and all values are in Å.

respectively, and the energy values include zero-point energy (ZPE) correction. When the CO molecule is adsorbed onto Ga in $[GaH]^{2+}$ through the C atom, the obtained value of E_{ads} is -112.9 kJ mol^{-1}, while through O adsorption the value is -74.7 kJ mol^{-1}. The E_{ads} values show that CO tends to adsorb on Ga through C adsorption, so C-end adsorption is used to study whether Ga can accept electrons.

We calculated the natural bond orbital (NBO) charge and listed the amount of charge transferred. The charge transfer values are shown in Table 1. For a single CO molecule, the values for C and O are 0.51 and -0.51 $|e|$, respectively. When CO is adsorbed on Ga in $[GaH]^{2+}$ of Ga-ZSM-5, the NBO charges on the C_{CO} and O_{CO} atoms are 0.59 and -0.33 $|e|$ in the complex, respectively; that is, the CO molecule bears a positive charge (0.26 $|e|$). At the same time, the NBO charge on Ga changes from 1.67 to 1.44 $|e|$ upon the formation of the CO-Ga-ZSM-5 complex; this indicates that electrons are transferred (0.23 $|e|$) from the CO molecule to Ga when CO is adsorbed on Ga. This result illustrates that Ga doped into ZSM-5 still has the ability to accept electrons.

Through the study of the methylcyclopentane to benzene process, it is found that the DH processes on H-Z_1 and H-Z_2 are the rate-determining steps and require high free energies for the formation of the target product. Ga-ZSM-5 promotes the production of benzene *via* greatly reducing the free energy required for DH. Therefore, we analyzed the reason why Ga-ZSM-5 can promote the DH process at the electronic level, as shown in Table 2. *Via* analyzing the NBO charges of H atoms producing H_2 on H-Z_1, H-Z_2, and Ga-ZSM-5, it is found that for H-Z_1 and H-Z_2, the H atoms of reactants and B-acid protons involved in the DH processes are all positive. However, for Ga-ZSM-5, the B acid involved in the DH process is positive, while the H atom of $[GaH]^{2+}$ is negative. This is attributed to Ga in $[GaH]^{2+}$ having the ability to accept electrons and donate the obtained electrons to the H atom of $[GaH]^{2+}$, so H presents a negative charge. As is well known, positively charged H and negatively charged H are easier to combine to produce H_2 than two positively charged H atoms. As Lisa *et al.*[33] mentioned, a negative species should be stabilized *via* interacting with a more positive species, which leads to the activation of specific chemical bonds. Our analysis is in good agreement with their results. Also, when the same mechanism and reaction processes are occurring on different catalysts, the greater the difference between the charges of the H atoms participating in producing H_2, the easier the DH reaction will occur.

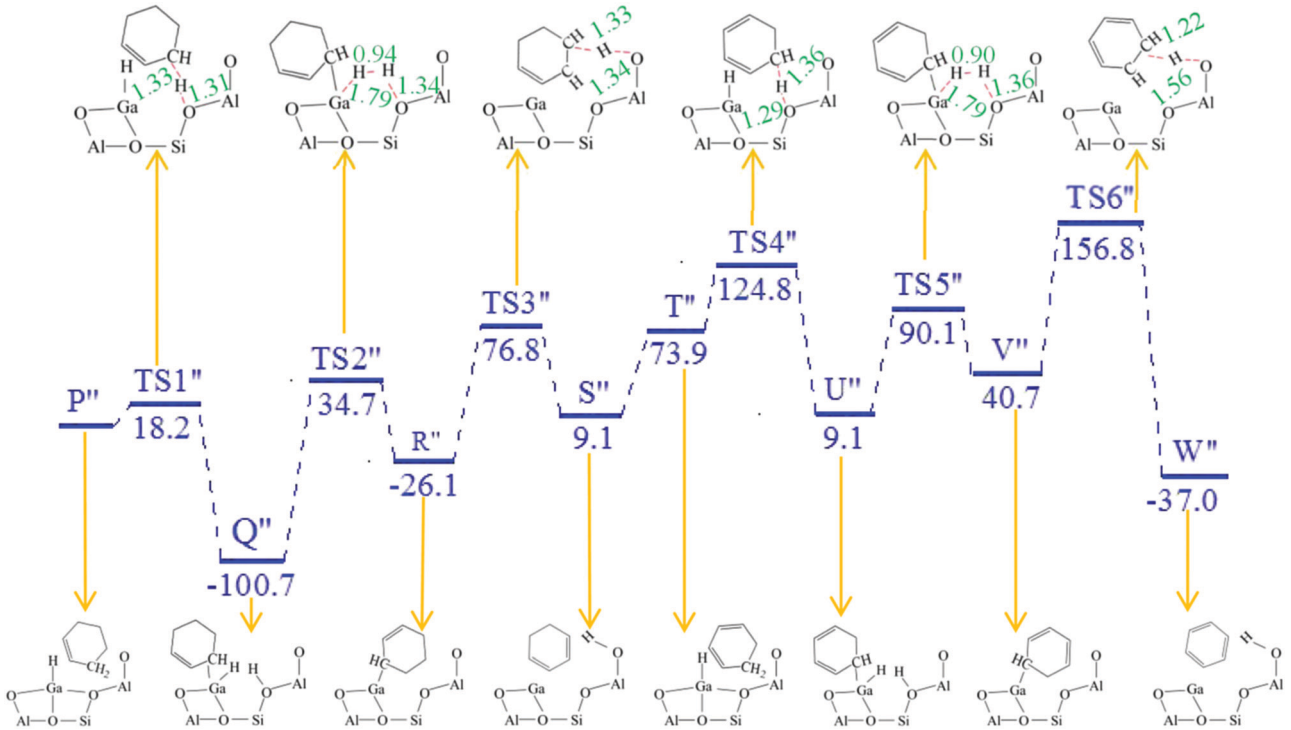

Fig. 16 The free energy barrier diagram of the cyclohexene to benzene process and the skeletal formulae of reactants, products, intermediates, and transition states on Ga-ZSM-5; all free energy values are in kJ mol^{-1}. The main geometric parameters of the transition states are also provided, and all values are in Å.

Table 1 NBO charges of C, O, and Ga of $[GaH]^{2+}$ in CO, Ga-ZSM-5, and their complex (units of |e|)

Species	CO	Ga-ZSM-5	Complex (C adsorption)
C_{CO}	0.51		0.59
O_{CO}	−0.51		−0.33
Ga of $[GaH]^{2+}$		1.67	1.44

3.4 Structural analysis of the transition states of the DH reaction

According to the calculation results, it can be seen that in the methylcyclopentane to benzene process, reducing the DH free energy barrier is the key to the formation of the target product.

Table 3 The bond distances of the transition states during the dehydrogenation of methylcyclopentane to benzene on H-Z_1

Catalyst	Bond distance (Å)	Transition state during the dehydrogenation of methylcyclopentane to benzene				
		P-TS1	S-TS1	T-TS1	TS1	TS3
H-Z_1	O–B acid	1.87	1.82	1.67	1.60	1.49
	B acid–H	0.77	0.78	0.79	0.81	0.84
	H–C	1.88	1.88	1.73	1.66	1.56

Previous reports usually clarified catalytic activities *via* analyzing the geometrical features of the transition states of key steps.[33,41] Based on this, we have carried out structural analysis of the transition states of all DH processes, including methylcyclopentane to

Table 2 NBO charges of H atoms producing H_2 on H-Z_1, H-Z_2, and Ga-ZSM-5 (units of |e|)

Catalyst	H atoms producing H_2	Methylcyclopentane			Cyclohexene	Cyclohexadiene
		Primary carbon mechanism	Secondary carbon mechanism	Tertiary carbon mechanism		
H-Z_1	B acid	0.58	0.58	0.58	0.58	0.58
	H of reactant	0.24	0.19	0.26	0.24	0.24
H-Z_2	B acid	0.58	0.57	0.57	0.58	0.58
	H of reactant	0.19	0.17	0.19	0.22	0.24
Ga-ZSM-5	B acid	0.58	0.58	0.58	0.58	0.58
	H of $[GaH]^{2+}$	−0.30	−0.32	−0.33	−0.30	−0.30

Table 4 The bond distances of the transition states during the dehydrogenation of methylcyclopentane to benzene on H-Z_2

Catalyst	Bond distance (Å)	Transition state during the dehydrogenation of methylcyclopentane to benzene				
		P-TS1′	S-TS1′	T-TS1′	TS1′	TS3′
H-Z_2	O–B acid	1.74	1.77	1.63	1.57	1.47
	B acid–H	0.79	0.79	0.80	0.82	0.85
	H–C	1.79	1.77	1.67	1.67	1.56

Table 5 The bond distances of the transition states during the dehydrogenation of methylcyclopentane to benzene on Ga-ZSM-5

Catalyst	Bond distance (Å)	Transition state during the dehydrogenation of methylcyclopentane to benzene				
		P-TS2″	S-TS2″	T-TS2″	TS2″	TS5″
Ga-ZSM-5	O–B acid	1.42	1.38	1.32	1.34	1.36
	B acid–H	0.87	0.90	0.95	0.94	0.90
	H–Ga	1.80	1.77	1.77	1.79	1.79

cyclohexene *via* primary, secondary, and tertiary carbon mechanisms, cyclohexene to cyclohexadiene, and cyclohexadiene to benzene on H-Z_1, H-Z_2, and Ga-ZSM-5, as shown in Tables 3–5, respectively. Compared with the H-C distances on H-Z_1 and H-Z_2, the H-Ga distance on Ga-ZSM-5 does not show any clear trend. This may be caused by the participation of H atoms from different species. However, the B acid-H distances on Ga-ZSM-5 are larger than those on H-Z_1 and H-Z_2, and the distances from the B acid to the ZSM-5 framework O atom on Ga-ZSM-5 are smaller than on H-Z_1 and H-Z_2. Combined with the result that Ga-ZSM-5 can promote the DH reaction, it can be seen that in the presence of Ga, B-acid protons can easily bind to H from Ga after leaving the framework O of ZSM-5, and when the distance between the two H atoms is large, they can combine to generate H_2. In contrast, for H-Z_1 and H-Z_2, the B-acid protons can form H_2 only when they are further from the framework O and closer to H from the reactant. This further proves that the introduction of Ga is beneficial to the DH reaction, which is highly consistent with the NBO charge analysis results given above.

4. Conclusions

Theoretical studies have been used to systematically investigate DH, HT, and ring expansion involved in the methylcyclopentane to benzene process, and the results show that DH is the rate-determining step on H-Z_1 and H-Z_2, requiring extremely high energy barriers and making it difficult for the reaction to proceed. Different from the DH process, the HT reaction is easy on H-Z_1 and H-Z_2. Calculation results indicate that HT is more difficult on Ga-ZSM-5 than on H-Z_1 and H-Z_2, but Ga-ZSM-5 significantly lowers the DH free energy barrier, making it more conductive for producing benzene.

NBO charge results show that Ga in the active center, $[GaH]^{2+}$, has the ability to withdraw electrons and donate the obtained electrons to a H atom of $[GaH]^{2+}$, making a H atom in $[GaH]^{2+}$ present negative charge. B-acid protons on Ga-ZSM-5 involved in DH processes relating to methylcyclopentane, cyclohexene, and cyclohexadiene are positive. Positively charged H and negatively charged H are easier to combine to produce H_2. In addition, analysis of the transition state structures of all DH processes also shows that Ga-ZSM-5 is better than H-Z_1 and H-Z_2 at promoting the combination of H for producing H_2.

Conflicts of interest

There are no conflicts to declare.

Acknowledgements

This work is financially supported by the Key Projects of the National Natural Science Foundation of China (No. 21736007), the National Natural Science Foundation of China (No. 21776193), Fund Program for the Scientific Activities of Selected Returned Overseas Professionals in Shanxi Province (No. 2017-14), Innovation & Application Engineering Research Center For Mesoporous Materials of Shanxi Provice (MMIA2019102), and Key R&D Projects of Datong (No. 218023).

References

1 J. H. Li, L. N. Wang, D. Zhang, J. H. Qian, L. Liu and J. J. Xing, *J. Fuel Chem. Technol.*, 2019, **47**, 957–963.
2 Y. M. Ni, A. M. Sun, X. L. Wu, G. L. Hai, J. G. Hu, T. Li and G. X. Li, *Microporous Mesoporous Mater.*, 2011, **143**, 435–442.
3 M. G. Ruiz, D. A. S. Casados, J. A. Pliego, C. M. Álvarez, E. S. de Andrés, D. S. Tartalo, R. S. Vaque and M. G. Casas, *React. Kinet., Mech. Catal.*, 2020, **129**, 471–490.
4 J. Kim, Mi Choi and R. Ryoo, *J. Catal.*, 2010, **269**, 219–228.
5 C. X. Xu, B. B. Jiang, Z. W. Liao, J. D. Wang, Z. L. Huang and Y. R. Yang, *RSC Adv.*, 2017, **7**, 10729–10736.
6 M. Guisnet, N. S. Gnep, D. Aittaleb and Y. J. Doyemet, *Appl. Catal., A*, 1992, **87**, 255–270.
7 J. L. Harris, N. Krisko and X. M. Wang, *Appl. Catal., A*, 1992, **83**, 59–74.
8 M. Vandichel, D. Lesthaeghe, J. V. D. Mynsbrugge, M. Waroquier and V. V. Speybroeck, *J. Catal.*, 2010, **271**, 67–78.
9 H. Ma, Y. Y. Chen, Z. H. Wei, S. Wang, Z. F. Qin, M. Dong, J. F. Li, J. G. Wang and W. B. Fan, *ChemPhysChem*, 2018, **19**, 496–503.
10 Y. Bi, Y. L. Wang, X. Chen, Z. X. Yu and L. Xu, *Chinese J. Catal.*, 2014, **35**, 1740–1751.
11 K. Wang, M. Dong, X. J. Niu, J. F. Li, Z. F. Qin, W. B. Fan and J. G. Wang, *Catal. Sci. Technol.*, 2018, **8**, 5646–5656.
12 Y. Gao, G. Wu, F. W. Ma, C. T. Liu, F. Jiang, Y. Wang and A. J. Wang, *Microporous Mesoporous Mater.*, 2016, **226**, 251–259.
13 K. Shen, W. Z. Qian, N. Wang, C. Su and F. Wei, *J. Mater. Chem. A*, 2014, **2**, 19797–19808.
14 M. Conte, J. A. Lopez-Sanchez, Q. He, D. J. Morgan, Y. Ryabenkova, J. K. Bartley, A. F. Carley, S. H. Taylor, C. J. Kiely, K. Khalid and G. J. Hutchings, *Catal. Sci. Technol.*, 2012, **2**, 105–112.

15 X. J. Niu, J. Gao, Q. Miao, M. Dong, G. F. Wang, W. B. Fan, Z. F. Qin and J. G. Wang, *Microporous Mesoporous Mater.*, 2014, **197**, 252–261.
16 Y. B. Xin, P. Y. Qi, X. P. Duan, H. Q. Lin and Y. Z. Yuan, *Catal. Lett.*, 2013, **143**, 798–806.
17 Z. Y. Chen, Y. M. Ni, Y. C. Zhi, F. L. Wen, Z. Q. Zhou, Y. X. Wei, W. L. Zhu and Z. M. Liu, *Angew. Chem., Int. Ed.*, 2018, **57**, 12549–12553.
18 J. Xu, Q. Wang and F. Deng, *Acc. Chem. Res.*, 2019, **52**, 2179–2189.
19 P. Gao, J. Xu, G. D. Qi, C. Wang, Q. Wang, Y. X. Zhao, Y. H. Zhang, N. D. Feng, X. L. Zhao, J. L. Li and F. Deng, *ACS Catal.*, 2018, **8**, 9809–9820.
20 Y. Inoue, K. Nakashiro and Y. Ono, *Microporous Mesoporous Mater.*, 1995, **4**, 379–383.
21 I. Pinilla-Herrero, E. Borfecchia, J. Holzinger, U. V. Mentzel, F. Joensen, K. A. Lomachenko, S. Bordiga, C. Lamberti, G. Berlier, U. Olsbye, S. Svelle, J. Skibsted and P. Beato, *J. Catal.*, 2018, **362**, 146–163.
22 X. J. Niu, J. Gao, K. Wang, Q. Miao, M. Dong, G. F. Wang, W. B. Fan, Z. F. Qin and J. G. Wang, *Fuel Process. Technol.*, 2017, **157**, 99–107.
23 T. Inui, H. Nagata, H. Matsuda, J. B. Kim and Y. Ishihara, *Ind. Eng. Chem. Res.*, 1992, **31**, 995–999.
24 V. R. Choudhary and P. Devadas, *J. Catal.*, 1997, **172**, 475–478.
25 V. R. Choudhary, P. Devadas, A. K. Kinage and M. Guisnet, *Appl. Catal., A*, 1997, **162**, 223–233.
26 P. Gao, Q. Wang, J. Xu, G. D. Qi, C. Wang, X. Zhou, X. L. Zhou, N. D. Feng, X. L. Liu and F. Deng, *ACS Catal.*, 2018, **8**, 69–74.
27 C. Y. Hsieh, Y. Y. Chen and Y. C. Lin, *Ind. Eng. Chem. Res.*, 2018, **57**, 7742–7751.
28 C. Mukarakate, K. Orton, Y. Kim, S. Dell Orco, C. A. Farberow, S. Kim, M. J. Watson, R. M. Baldwin and K. A. Madrini, *ACS Sustainable Chem. Eng.*, 2020, **8**, 2652–2664.
29 G. Fogassy, N. Thegarid, Y. Schuurman and C. Mirodatos, *Energy Environ. Sci.*, 2011, **4**, 5068–5076.
30 Y. Y. Chu, X. F. Yi, C. B. Li, X. Y. Sun and A. M. Zheng, *Chem. Sci.*, 2018, **9**, 6470–6479.
31 H. Ma, Y. Sun, J. P. Yu, J. R. Qiao, W. Y. Jin, G. J. Kang, Y. L. Wang and J. Ma, *Microporous Mesoporous Mater.*, 2020, **294**, 109838.
32 T. X. Chen, B. L. Huang, S. Day, C. C. Tang, S. C. E. Tsang, K. Y. Wong and T. W. B. Lo, *Angew. Chem., Int. Ed.*, 2019, **132**, 1109–1113.
33 K. Lisa, Y. Kim, K. A. Orton, D. J. Robichaud, R. Katahira, M. J. Watson, E. C. Wegener, M. R. Nimlos, J. A. Schaidle, C. Mukarakate and S. Kim, *Green Chem.*, 2020, **22**, 2403.
34 N. Hansen, T. Kerber, J. Sauer, A. T. Bell and F. J. Keil, *J. Am. Chem. Soc.*, 2010, **132**, 11525–11538.
35 D. Wang, C. M. Wang, G. Yang, Y. J. Du and W. M. Yang, *J. Catal.*, 2019, **374**, 1–11.
36 Z. H. Wen, T. F. Xia, M. H. Liu, K. K. Zhu and X. D. Zhu, *Catal. Commun.*, 2016, **75**, 45–49.
37 N. Rane, A. R. Overweg, V. B. Kazansky, R. A. van Santen and E. J. M. Hensen, *J. Catal.*, 2006, **239**, 478–485.
38 M. W. Schreiber, C. P. Plaisance, M. Baumgartl, K. Reuter, A. Jentys, R. Bermejo-Deval and J. A. Lercher, *J. Am. Chem. Soc.*, 2018, **140**, 4849–4859.
39 N. M. Phadke, J. Van der Mynsbrugge, E. Mansoor, A. B. Getsoian, M. Head-Gordon and A. T. Bell, *ACS Catal.*, 2018, **8**, 6106–6126.
40 Y. V. Joshi and K. T. Thomson, *J. Catal*, 2007, **246**, 249–265.
41 E. Mansoor, M. Head-Gordon and A. T. Bell, *ACS Catal.*, 2018, **8**, 6146–6162.
42 X. W. Nie, M. J. Janik, X. W. Guo and C. S. Song, *J. Phys. Chem. C*, 2012, **116**, 4071–4082.
43 T. Vreven and K. Morokuma, *J. Comput. Chem.*, 2000, **21**, 1419–1432.
44 Y. V. Joshi, A. Bhan and K. T. Thomson, *J. Phys. Chem. B*, 2004, **108**, 971–980.
45 Y. V. Joshi and K. T. Thomson, *J. Mol. Catal*, 2005, **230**, 440–463.
46 D. H. Liu and C. L. Zhong, *J. Phys. Chem. Lett.*, 2010, **1**, 97–101.
47 L. Benco, T. Bucko, J. Hafner and H. Toulhoat, *J. Phys. Chem. B*, 2004, **108**, 13656–13666.
48 S. J. Jiang, S. P. Huang, W. X. Tu and J. Q. Zhu, *Appl. Surf. Sci.*, 2009, **255**, 5764–5769.